J. Pestic. Sci. **47**(2), 78–85 (2022)
DOI: 10.1584/jpestics.D22-007

JOURNAL OF PESTICIDE SCIENCE

Regular Article

Structural insights into the interaction between gabazine (SR-95531) and *Laodelphax striatellus* GABA receptors

Yuki Fujie,[1] Genyan Liu,[2,*] Fumiyo Ozoe[3] and Yoshihisa Ozoe[1,3,*]

[1] *Faculty of Life and Environmental Sciences, Shimane University, Matsue, Shimane 690–8504, Japan*
[2] *Key Laboratory for Green Chemical Process of Ministry of Education, School of Chemical Engineering and Pharmacy, Wuhan Institute of Technology, Wuhan, Hubei 430205, People's Republic of China*
[3] *Interdisciplinary Institute for Science Research, Organization for Research and Academic Information, Shimane University, Matsue, Shimane 690–8504, Japan*

(Received February 23, 2022; Accepted April 13, 2022)

Supplementary material

γ-Aminobutyric acid receptors (GABARs) mediate fast inhibitory neurotransmission and are targets for insecticides. GABARs are composed of five subunits, the composition of which dictates the pharmacological characteristics of GABARs. Both competitive and noncompetitive GABAR antagonists can be used as insecticides. Gabazine is a potent competitive antagonist of mammalian $\alpha1\beta2\gamma2$ GABARs; however, it is less potent against insect GABARs. To explore how gabazine interacts with GABARs, we examined whether the sensitivity of the small brown planthopper (*Laodelphax striatellus*) RDL GABAR (LsRDLR) to gabazine is increased when its amino acid residues are substituted with $\alpha1\beta2\gamma2$ GABAR residues. In the results, two of the generated mutants showed enhanced gabazine sensitivity. Docking simulations of gabazine using LsRDLR homology models and an $\alpha1\beta2\gamma2$ GABAR cryo-EM structure revealed that the accommodation of gabazine into the "aromatic box" in the orthosteric site lowered the binding energy. This information may help in designing GABAR-targeting insecticides with novel modes of action.

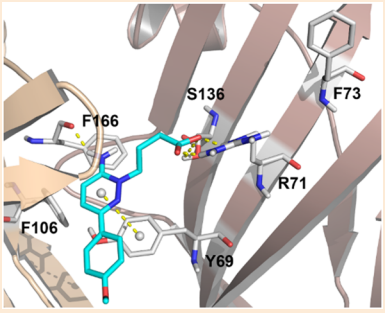

Keywords: γ-aminobutyric acid, GABA receptor, insecticide, competitive antagonist, gabazine, small brown planthopper.

Introduction

γ-Aminobutyric acid (GABA) is a fast inhibitory neurotransmitter that plays a vital role in various physiological processes in animals.[1,2] GABA binds to GABA receptors (GABARs) and stabilizes the resting potential of a cell by increasing chloride conductance through the cell membrane.[3] This action negates the membrane depolarization caused by excitatory neurotransmitters, such as L-glutamate and acetylcholine. GABARs are membrane-embedded GABA-activated chloride channels consisting of five subunits assembled to form an ionophore at the center.[4] Human type A GABARs ($GABA_A$Rs) are hetero- or homopentamers with five subunits selected from a repertoire of 19 subunits ($\alpha1$–6, $\beta1$–3, $\gamma1$–3, δ, ε, θ, π, and $\rho1$–3).[4,5] The stoichiometry of the major $GABA_A$R in the brain is $(\alpha1)_2(\beta2)_2(\gamma2)_1$. Predominant insect GABARs are most likely homopentamers constituted of five RDL subunits,[6,7] hereafter referred to as RDLRs. The composition and arrangement of subunits dictate the physiological and pharmacological characteristics of GABARs.

Insect GABARs are important targets for existing insecticides, such as fiproles, broflanilide, and fluxametamide.[8–10] These insecticides are broadly categorized as noncompetitive antagonists that inhibit GABA-activated chloride conductance by binding to either a site within the channel (fiproles) or a site in the transmembrane subunit interface (broflanilide and fluxametamide). Additionally, RDLRs contain unutilized promising target sites for insecticidal compounds, such as the orthosteric agonist-binding site, which exists at the extracellular subunit interface of adjacent subunits. Competitive antagonists bind to the orthosteric site, thereby leading to a closed-channel state of GABARs as with noncompetitive antagonists,[11] indicating that competitive antagonists may be utilized as insecticides. However, little information is available regarding competitive antagonists that

* To whom correspondence should be addressed.
E-mail: liugenyan@wit.edu.cn, ozoe-y@life.shimane-u.ac.jp
Published online May 18, 2022

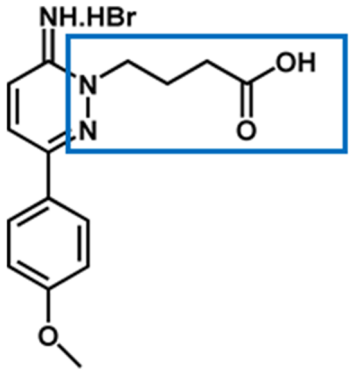

Fig. 1. Chemical structure of gabazine (SR-95531). The GABA structural scaffold is boxed.

are effective against insect GABARs. We previously reported that gabazine (SR-95531) (Fig. 1), a competitive antagonist of $\alpha1\beta2\gamma2$ GABARs, inhibits the GABA response in the RDLRs of the small brown planthopper *Laodelphax striatellus* (*striatella*).[12] Structure–activity studies of gabazine and its analogs may provide clues for the discovery of novel insecticides. It is challenging to identify highly potent competitive antagonists against insect GABARs.[13] In the present study, we aimed to provide a basis for the design of novel insecticides by exploring the interaction between gabazine and amino acid residues in the orthosteric site of *L. striatellus* RDLR (LsRDLR) using site-directed mutagenesis, electrophysiology, and ligand-docking simulation.

Materials and methods

1. Chemicals

Gabazine [SR-95531, 2-(3-carboxypropyl)-6-(4-methoxyphenyl)-2,3-dihydropyridazin-3-iminium bromide] was purchased from Fujifilm Wako Pure Chemical (Osaka, Japan). Other chemicals were purchased from Sigma-Aldrich Japan (Tokyo, Japan) and Fujifilm Wako Pure Chemical, unless otherwise noted.

2. cDNAs encoding L. striatellus *RDL subunits*

The plasmid vector pcDNA3.2/V5-DEST-*LsRdl* constructed in our previous study[12] was used to express wild-type (WT) *L. striatellus* RDLRs (LsRDLRs). A Quikchange Site-Directed Mutagenesis Kit (Agilent Technologies Japan, Tokyo, Japan) was used to generate *LsRdl* cDNAs. The oligonucleotide primers used for mutagenesis are listed in Table S1.

3. Two-electrode voltage clamp (*TEVC*) *electrophysiology*

The cDNA template, which includes *LsRdl* (accession no. AB253526) and the T7 RNA polymerase promoter site located upstream of *LsRdl*, was amplified from pcDNA3.2/V5-DEST-*LsRdl* by PCR using the primers pcDNA3-F1 and attB2-r (Table S1) and KOD-Plus-DNA polymerase (Toyobo, Osaka, Japan). The PCR products were purified using the GFX PCR DNA and Gel Band Purification Kit (Cytiva, Tokyo, Japan) and validated by sequence analysis. Poly(A) cRNAs were synthesized using the cDNA template and T7 RNA polymerase included in the mMESSAGE mMACHINE T7 Ultra Kit (Thermo Fisher Scientific, Waltham, MA, USA), purified by LiCl precipitation, and dissolved in sterile RNase-free water at a concentration of 543 ng/nL. The cDNA templates of mutants were similarly prepared.

Mature female African clawed frogs (*Xenopus laevis*) purchased from Shimizu Laboratory Supplies (Kyoto, Japan) were immersed in 0.1% tricaine methylate for 30 min to induce anesthesia. Ovarian lobes were surgically removed and treated with *Clostridium histolyticum* collagenase (2 mg/mL) in Ca^{2+}-free standard oocyte solution (SOS) (100 mM NaCl, 2 mM KCl, 1 mM $MgCl_2$, 5 mM HEPES, pH 7.6) at ambient temperature for 90–120 min. The oocytes were gently washed with Ca^{2+}-free SOS and transferred into SOS (100 mM NaCl, 2 mM KCl, 1.8 mM $CaCl_2$, 1 mM $MgCl_2$, 5 mM HEPES, pH 7.6) containing gentamicin (50 μg/mL), penicillin (100 units/mL), streptomycin (100 μg/mL), and sodium pyruvate (2.5 mM), and then incubated at 16°C overnight. Each oocyte was injected with 5 ng of cRNA dissolved in RNase-free water (9.2 nL) and then incubated in SOS at 16°C for 48 hr.

Electrophysiological experiments were performed using an Oocyte Clamp OC-725C amplifier (Warner Instruments, Holliston, MA, USA) at a holding potential of −80 mV. The data were digitized using Lab-Trax-4-16 software (World Precision Instruments, Sarasota, FL, USA) and analyzed using DataTrax2 (World Precision Instruments). The glass microelectrodes with 1.5–2.0 MΩ (for monitoring voltage) and 0.5–1.0 MΩ (for injecting current) were filled with 2 M KCl. The oocytes were placed in a recording bath that was continuously perfused with SOS at 18–20°C. GABA dissolved in SOS was applied to the oocytes for 3 sec at intervals of 30–60 sec to ensure full recovery from desensitization. SOS containing gabazine was perfused after two successive control applications of GABA (EC_{50}); the concentrations used are shown in Table S2. After perfusing gabazine solution alone for 30 sec, GABA was coapplied with gabazine for 3 sec at a concentration close to the EC_{50} value for each GABAR type. Coapplication was repeated at 30-s intervals until steady-state inhibition was reached. In each oocyte, the GABA responses in the presence of gabazine were normalized to the control current induced by GABA alone. Each experiment was performed using at least six oocytes obtained from at least two frogs. EC_{50} values were obtained by fitting a four-parameter logistic equation to the concentration-response curves between 0 and 100% with a variable slope using OriginPro (LightStone, Tokyo, Japan) and are presented as the mean±S.D.

4. Homology modeling

The LsRDLR homology model was constructed using the cryo-electron microscopy (cryo-EM) structure of human $\alpha1\beta2\gamma2$ GABAR (PDB ID: 6X3S) as a template. The amino acid sequence of the WT LsRDL subunit (UniProt ID: AB253526) was retrieved from UniProtKB (http://www.uniprot.org/). Suitable template proteins were searched using the SWISS-MODEL server (https://swissmodel.expasy.org/interactive) by uploading the

sequence of the target protein. As the intracellular loop of the TM3–TM4 region (α1: K339–S417, β2: N327–N485, γ2: S361–A439) was replaced by the SQPARAA segment in the template, the same procedure was performed to model the LsRDLR. Sequence alignment was performed using ClustalW (https://www.genome.jp/tools-bin/clustalw) to compare the template and target sequences. Alignment results were generated using the ESPript website (http://espript.ibcp.fr/ESPript/cgi-bin/ESPript.cgi). Finally, the LsRDLR model was built using the SWISS-MODEL server.

To fix potential errors such as unreasonable bond lengths, bond angles, and dihedrals in the initial model, the modeled protein was further energy minimized under an AMBER7 FF99 force field using SYBYL-X 2.1 software (Tripos Inc., St. Louis, MO, USA) running on a Windows 7 workstation. The optimized model was validated using the SAVES server to check its quality (https://saves.mbi.ucla.edu/). A reasonable model was used for the subsequent molecular docking.

5. Computational mutations

Mutations in the constructed LsRDLR model were generated using the Mutate Monomers module of SYBYL-X 2.1 software. In the same manner as in the WT model, these mutant models were energy minimized under an AMBER7 FF99 force field with a gradient convergence criterion of 0.05 kcal/mol/Å in the Compute module. The optimized mutants were used in subsequent studies.

6. Molecular docking

The structure of gabazine was sketched in SYBYL-X 2.1 and energy minimized under Tripos force field with Gasteiger–Hückel charges. Docking simulations were performed using the Surflex-Dock module in SYBYL-X 2.1 software. Gabazine was docked with a carboxyl group in its dissociated form and an imino group in its protonated form. The gradient convergence criterion was set to 0.005 kcal/mol/Å, and the maximum iteration coefficient was set to 1000. Other parameters were set to the default values. Y69 (F69), R71, F106 (Y106), E164, S165, F166, Y214, and R216 amino acid residues of LsRDLR were selected to generate the applicable binding pocket in residue mode using the Surflex-Dock Geom module. Twenty conformations of gabazine with different docking scores were obtained, and the one with the highest score and a suitable binding pattern was selected for analysis. PyMOL software (DeLano Scientific, San Carlos, CA, USA) was used to visualize the docking results.

Surflex-Dock employs an empirical scoring function, which is based on the binding affinities of protein-ligand complexes and on their X-ray structures, and a patented search engine to dock ligands into a protein-binding site.[14–16] The Surflex-Dock scoring function is a weighted sum of nonlinear functions involving van der Waals surface distances between the appropriate pairs of exposed protein and ligand atoms.[15] The total scores, expressed in $-\log K_d$ units, are generated automatically by SYBYL-X 2.1 software (Eq. 1).[15] The binding free energies (ΔG, kcal/mol), which reflect the binding affinity of gabazine for LsRDLRs, were calculated from the docking total scores using Eqs. 1 and 2, where K_d is the dissociation constant, and RT is equal to 0.59 kcal/mol.

$$\text{Total score} = -\log K_d \quad (1)$$

$$\Delta G = RT \ln K_d \quad (2)$$

Results

1. Sensitivity of WT and mutant LsRDLRs to gabazine

The orthosteric site of GABARs, which is the binding site for agonists and competitive antagonists, is formed by six loops (A–F) in the N-terminal extracellular domain interface between the principal and complementary subunits.[4] Loops A–C originate from the principal subunit, and loops D–F originate from the complementary subunit. To examine whether the gabazine sensitivity of LsRDLR is enhanced by substituting its amino acid residues with the residues of $\alpha1\beta2\gamma2$ GABAR, which is sensitive to gabazine, we generated seven mutants, including those with single, double, and triple mutations for two residues (Y69 and F73) in loop D and one residue (F106) in loop A (Fig. 2, Table 1). Using TEVC electrophysiology, we first examined whether functional LsRDLR mutants are expressed in *Xenopus* oocytes. Consequently, we confirmed that all LsRDLRs, including the WT (Fig. 3a) and Y69F mutant (Fig. 3b), which was the least sensitive, showed robust responses to GABA. The EC_{50} values obtained from concentration–response curves (Fig. 3c) ranged from 4 to 130 μM, and Hill coefficients ranged from 1.7 to 2.5 (Table 1).

Next, we examined the inhibitory effects of gabazine (30 μM) on currents induced by the approximate EC_{50} (Table S2) of GABA in WT and mutant LsRDLRs. As shown in Fig. 4c, gabazine suppressed GABA responses to 77.8±8.0% (mean±

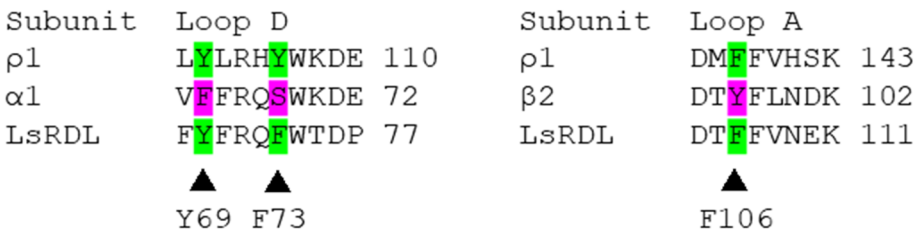

Fig. 2. Sequence alignment of loops D and A of ρ1, α1, and LsRDL subunits. The amino acid numbering in LsRDLR starts at the cleavage site (the 23rd residue from the initiating M) determined using the SignalP 6.0 server (https://services.healthtech.dtu.dk/service.php?SignalP).

Table 1. GABA response profiles of WT and mutant LsRDLRs expressed in *Xenopus* oocytes

LsRDLR type	EC_{50} (μM)[a]	Hill coefficient[a]	*n*
WT	6.83±3.74	2.47±0.33	14
Y69F	131±45	1.83±0.19	7
F73S	4.08±1.31	2.02±0.53	6
F106Y	43.7±10.2	2.44±0.34	6
Y69F/F73S	63.2±23.8	2.25±0.61	6
Y69F/F106Y	37.3±11.8	2.49±1.10	7
F73S/F106Y	25.6±11.9	1.89±0.44	6
Y69F/F73S/F106Y	15.4±3.7	1.70±0.48	6

[a]Data are presented as the mean±S.D. of 6–14 independent experiments.

S.D., n=6) in WT LsRDLRs. In single mutants, gabazine exhibited no or a marginal inhibitory effect on GABA responses. In the F73S/F106Y double mutant, however, gabazine reduced GABA responses to 45.2±3.4% (mean±S.D., n=6), which was a greater reduction in current amplitude than that in the WT (p<0.05, unpaired t-test); gabazine did not significantly affect the GABA responses of the other double mutants (Fig. 4a, c). The introduction of an additional substitution (Y69F) to this double mutant resulted in the Y69F/F73S/F106Y triple mutant, which had enhanced gabazine sensitivity compared with that of the WT (p<0.05, unpaired t-test) but no higher sensitivity than the F73S/F106Y mutant, with relative responses of 34.6±10.6% (mean±S.D., n=6) (Fig. 4b, c).

2. Docking simulation of gabazine

To investigate the mechanism underlying the increased gabazine sensitivity in the F73S/F106Y and Y69F/F73S/F106Y mutants, we performed docking simulations of gabazine using seven mutant LsRDLR homology models and a WT model. The models were constructed using a recently published cryo-EM structure of human $\alpha1\beta2\gamma2$ GABAR bound to bicuculline,[17] a competitive $\alpha1\beta2\gamma2$ GABAR antagonist, as a template. Additionally, we performed a similar docking simulation using the $\alpha1\beta2\gamma2$ GABAR cryo-EM structure to compare the gabazine binding profiles of insect and mammalian GABARs.

2.1. Docking of gabazine into the WT LsRDLR homology model and $\alpha1\beta2\gamma2$ GABAR cryo-EM structure

We first performed docking simulations of gabazine in WT LsRDLR and $\alpha1\beta2\gamma2$ GABAR. The docking results showed that Y69 (loop D) of the complementary subunit in WT LsRDLR interacted with the iminodihydropyridazine ring of gabazine through π–π stacking (Fig. 5a). F166 (loop B) served as a hydrogen bond acceptor (backbone C=O) but not as a π–π stacking partner. The docking pose of gabazine in $\alpha1\beta2\gamma2$ GABAR was similar to that previously reported.[18] In $\alpha1\beta2\gamma2$ GABAR, the residue (F65) corresponding to the Y69 of LsRDLR similarly interacted with the phenyl group through π–π stacking (Fig. 5b). Further, Y157 (loop B) of the principal subunit interacted with the iminodihydropyridazine ring through π–π stacking. The association of F65 of the $\alpha1$ subunit of $\alpha1\beta2\gamma2$ GABAR with the gabazine binding site agrees with previously reported results.[19] Additionally, Y157 (backbone C=O) and Y205 (loop C) of $\alpha1\beta2\gamma2$ $GABA_AR$ stabilized the binding by forming hydrogen bonds with the imino group of the dihydropyridazine ring (Fig.

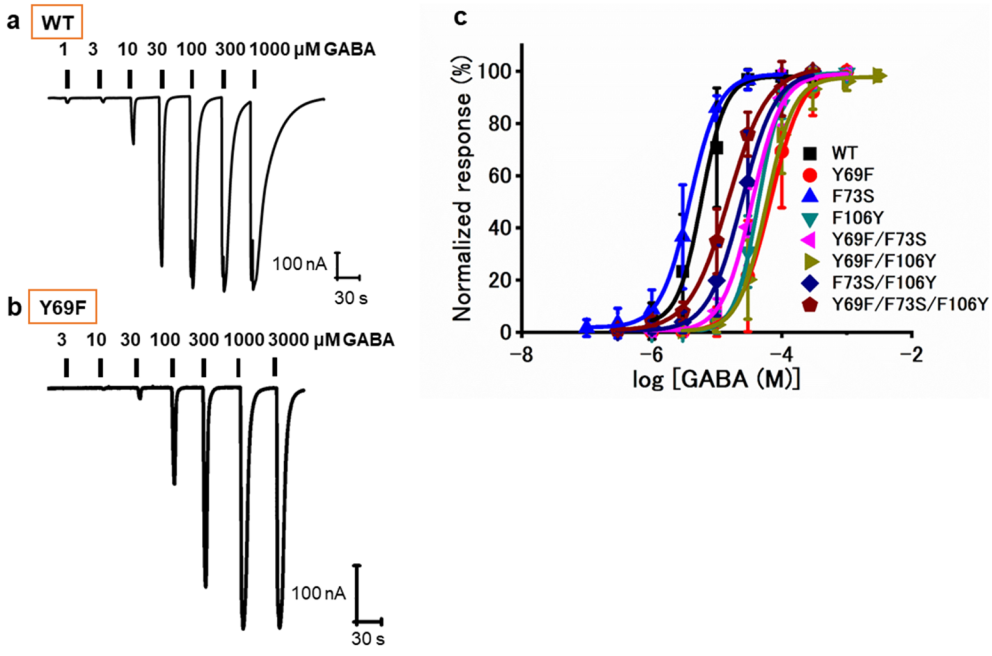

Fig. 3. GABA responses of LsRDLRs. (a) A trace of GABA-induced current in the WT. (b) A trace of GABA-induced current in the Y69F mutant. (c) GABA concentration–response curves for all tested LsRDLRs.

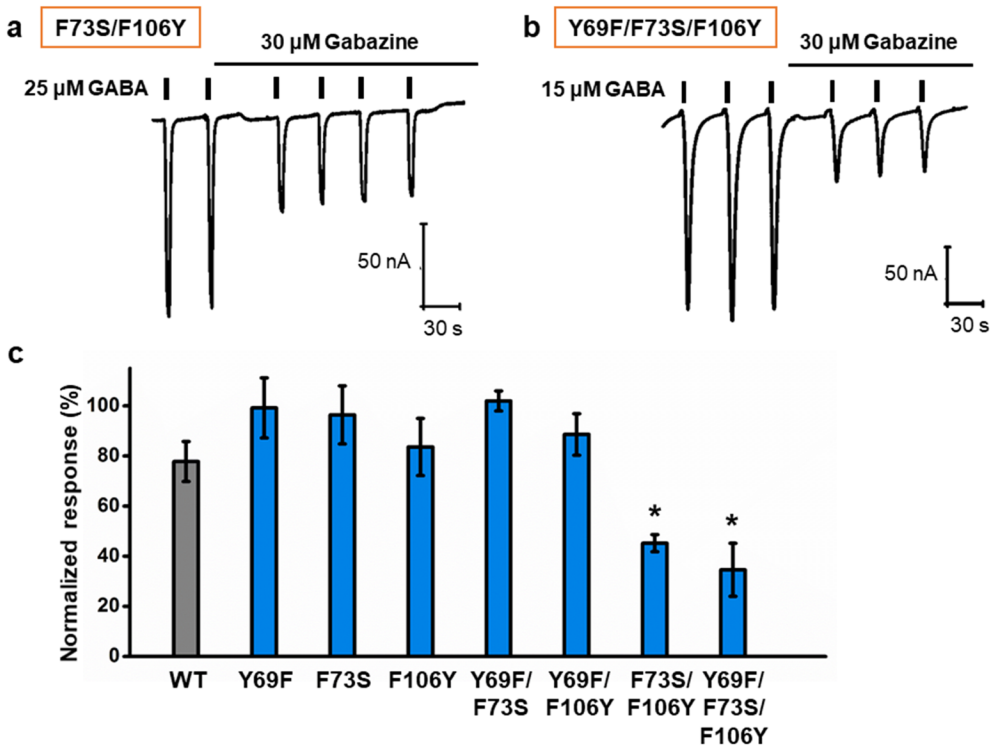

Fig. 4. Effects of gabazine on WT and mutant LsRDLRs. (a) Effects of 30 μM gabazine on GABA-induced current in the F73S/F106Y double mutant. (b) Effects of 30 μM gabazine on GABA-induced current in the Y69F/F73S/F106Y triple mutant. (c) Effects of 30 μM gabazine on GABA responses in WT and mutant LsRDLRs. Data are the mean±S.D. of 6 replicates. * $p<0.05$ (unpaired *t*-test relative to the WT).

5b). Two residues of the complementary subunit, R71 (loop D) and S136 (loop E), interacted with the carboxyl group of gabazine *via* hydrogen bonding in WT LsRDLR (Fig. 5a), whereas R67 and R120 formed hydrogen bonds with the carboxyl group in $\alpha1\beta2\gamma2$ GABAR (Fig. 5b). R67 is the residue that interacts with the carboxyl group of GABA.[20] Three arginines, including R67, reportedly play unique roles in binding gabazines.[21]

Czajkowski and coworkers performed intensive studies to identify residues that directly or indirectly interact with gabazine in the orthosteric site of rat $\alpha1\beta2$ or $\alpha1\beta2\gamma2$ GABAR using the substituted cysteine accessibility method.[22–26] The identified residues include D62, F64, and R66 ($\alpha1$ loop D)[22]; Y97 and L99 ($\beta2$ loop A)[23]; R119 ($\alpha1$ loop E)[24]; V178, V180, and D183 ($\alpha1$ loop F)[25]; and S204, Y205, R207, and S209 ($\beta2$ loop C)[26]; note that residue numbers in rat $\alpha1$ are smaller than those in human $\alpha1$ by one, although numbers in rat and human $\beta2$ are the same. Of these, four residues (F64, R66, R119, and Y205) agreed with those that were indicated to directly interact with gabazine in our model (Fig. 5b). Overall, our findings suggest that multiple noncovalent bond interactions between gabazine and $\alpha1\beta2\gamma2$

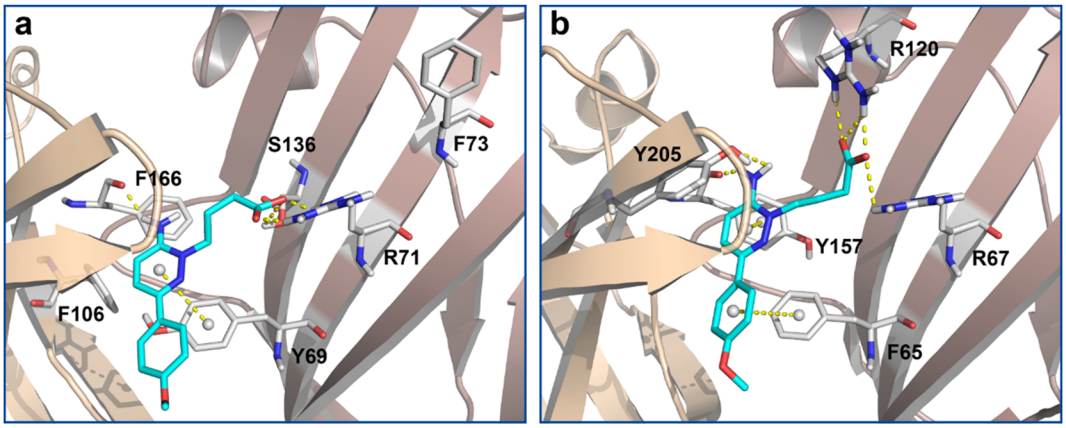

Fig. 5. Docking of gabazine into (a) the WT LsRDLR homology model and (b) cryo-EM structure of human $\alpha1\beta2\gamma2$ GABAR (PDB ID: 6X3S). F65 and R67 of $\alpha1\beta2\gamma2$ GABAR correspond to Y69 and R71 of LsRDLR, respectively.

Table 2. Binding energies and intermolecular forces in gabazine docking into LsRDLR homology models and the human $\alpha1\beta2\gamma2$ GABAR cryo-EM structure

GABAR	Binding energy (kJ/mol)	Hydrogen bond	π–π Stacking
LsRDLR			
WT	−38.4	$F166^{B}$, $R71^{D}$, $S136^{E}$	$Y69^{D}$
$Y69^{D}F$	−37.8	$S165^{B}$, $F166^{B}$, $S136^{E}$	$F69^{D}$
$F73^{D}S$	−39.0	$S165^{B}$, $F166^{B}$, $R71^{D}$	$Y69^{D}$
$F106^{A}Y$	−36.3	$S165^{B}$, $F166^{B}$, $R71^{D}$	$Y69^{D}$
$Y69^{D}F/F73^{D}S$	−36.2	$F166^{B}$, $R126^{E}$	$F69^{D}$
$Y69^{D}F/F106^{A}Y$	−37.3	$F166^{B}$, $R71^{D}$, $R126^{E}$, $S136^{E}$	$F69^{D}$
$F73^{D}S/F106^{A}Y$	−41.5	$F166^{B}$, $R71^{D}$	$Y69^{D}$
$Y69^{D}F/F73^{D}S/F106^{A}Y$	−40.2	$S165^{B}$, $F166^{B}$, $T211^{C}$, $S136^{E}$	$F69^{D}$
Human GABAR			
$\alpha1\beta2\gamma2$ GABAR cryo-EM	−47.3	$Y157^{\beta B}$, $Y205^{\beta C}$, $R67^{\alpha D}$, $R120^{\alpha E}$	$Y157^{\beta B}$, $F65^{\alpha D}$

Superscript uppercase letters indicate loop names. Superscript Greek letters indicate subunit names.

GABAR result in remarkably low binding energy (−47.3 kJ/mol) as compared with that of WT LsRDLR (−38.4 kJ/mol) (Table 2).

2.2. Docking of gabazine into the homology models of mutant LsRDLRs

Introducing a single mutation—F73S or F106Y—into the WT created a hydrogen bond between the protonated imino group and S165 (backbone C=O) and changed the π–π stacking interaction of Y69 with the iminodihydropyridazine ring to interact with the phenyl group (Fig. 6a, b). The introduction of the double mutation F73S/F106Y eliminated the hydrogen bond with S165 (Fig. 6c). Importantly, this mutation resulted in a lower binding energy (−41.5 kJ/mol) than those of the single mutants

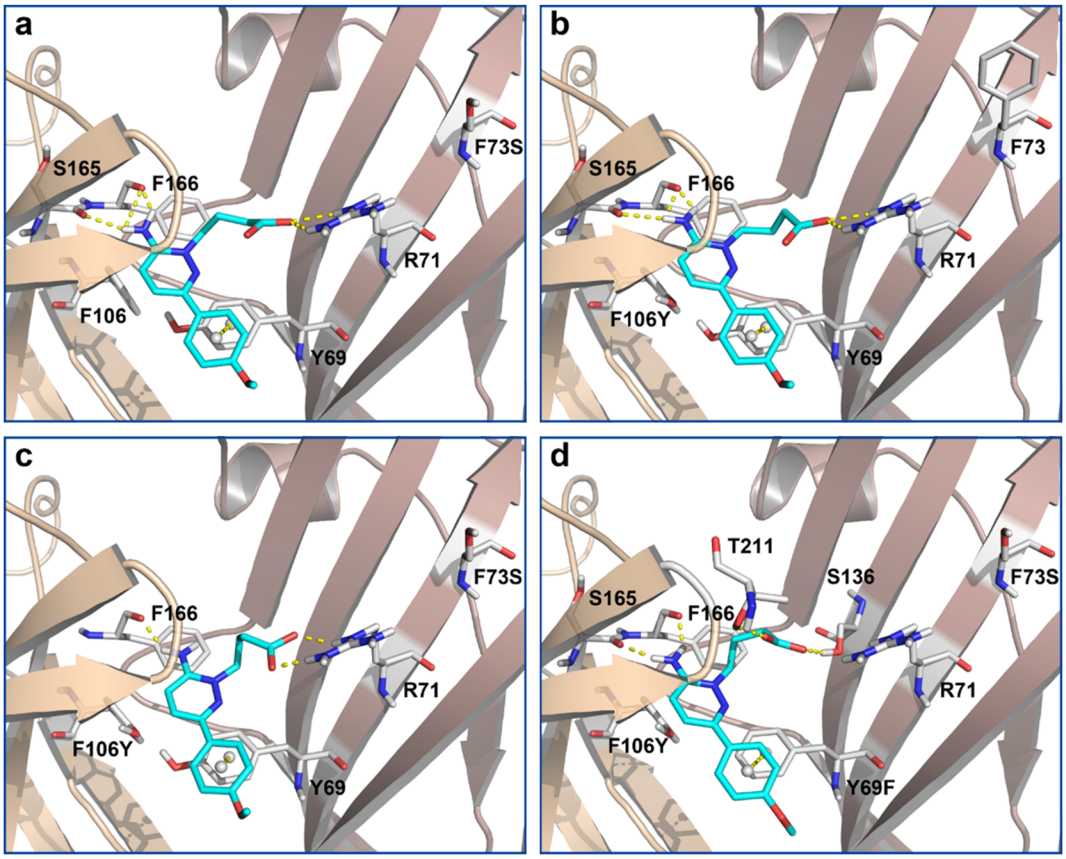

Fig. 6. Docking of gabazine into LsRDLR homology models. (a) F73S mutant model. (b) F106Y mutant model. (c) F73S/F106Y mutant model. (d) Y69F/F73S/F106Y mutant model.

(Table 2); this is consistent with the enhanced sensitivity of this mutant to gabazine. The binding energies of the other double mutants, which were insensitive to gabazine, were higher than that of this mutant (Table 2; see Fig. S1 for the docking poses of gabazine-insensitive mutants). Because the Y69F mutation resulted in the elimination of hydrogen bonding with R71 and the generation of hydrogen bonding with S136 (Fig. S1a), adding the Y69F mutation to the F73S/F106Y mutant led to the recovery of a hydrogen bond with S165 and the creation of a hydrogen bond with T211 (Fig. 6d). This resulted in the second-lowest binding energy (−40.2 kJ/mol) in LsRDLRs (Table 2), which agrees with the enhanced gabazine sensitivity of the triple mutant.

Discussion

Insect GABARs are unique in nature but pharmacologically resemble mammalian homomeric ρ1 GABARs rather than heteromeric $\alpha1\beta2\gamma2$ GABARs.[6] For example, *cis*-4-aminocrotonic acid, a ρ1 GABAR-selective agonist, activates currents in insect GABARs.[12,27,28] Bicuculline, a competitive antagonist selective for $\alpha1\beta2\gamma2$ $GABA_A$Rs, is ineffective in both insect and ρ1 GABARs.[29–31] Gabazine potently inhibits $\alpha1\beta2\gamma2$ GABAR but is less potent against both insect and ρ1 GABARs.[12,27,31] Zhang *et al.* performed a comparative pharmacological analysis of ρ1 and $\alpha1\beta2\gamma2$ GABARs to identify which amino acid residues of ρ1 GABAR lower its sensitivity to gabazine and bicuculline. The analysis used GABAR mutants, ρ1 GABAR with several residues replaced by the corresponding residues of $\alpha1\beta2\gamma2$ GABAR or vice versa.[31] Consequently, they found that Y102F, Y106S, F138Y, and Y106S/F138Y substitutions enhanced the sensitivity of ρ1 GABAR to gabazine, indicating that Y102, Y106, and F138 are responsible for the low potency of gabazine against ρ1 GABAR (Fig. 2). Furthermore, docking simulation led to speculation that Y102F and F138Y substitutions enable hydrophobic interactions and hydrogen bonding with gabazine, respectively. Although the Y106S mutation occurs away from the binding site, it was predicted that the docked gabazine approaches the residue in ρ1 GABAR by rotation in this mutant.

We investigated whether a similar enhancement occurs in LsRDLR mutants and consequently found that F73S/F106Y and Y69F/F73S/F106Y mutants are more sensitive to gabazine than is the WT. To gain insights into the mechanism of the enhancement of sensitivity in LsRDLRs, we performed a docking simulation of gabazine using homology models. The results of our simulation showed that gabazine binds to the F73S/F106Y mutant with a low binding energy. Although the number of hydrogen bonds between gabazine and the double mutant decreased compared with the number in single mutants, the binding energy of this mutant was lowered because the binding energy originates from total interactions based on hydrophobicity, polarity, repulsion, entropy, solvation, crash, *etc*. The F73S/F106Y mutation might reduce molecular constraints in the gabazine binding, but it has yet to be determined what intramolecular forces are responsible for the decline in the binding energy. The residue at the 69-position, either Y or F, is involved in π–π interactions with gabazine; Y(F)69 corresponds to the residues reported to interact with GABA, bicuculline, and gabazine in other GABARs.[19,22,32] However, neither the residues at the 73-position nor those at the 106-position directly interacted with gabazine in LsRDLR. These findings indicate that the enhancement of gabazine sensitivity by F73S/F106Y and Y69F/F73S/F106Y mutations in LsRDLRs may be caused by conformational changes in the orthosteric binding site, albeit not drastic, rather than by direct interaction with gabazine.

In conclusion, although the substitution of LsRDLR amino acid residues with the corresponding residues of $\alpha1\beta2\gamma2$ GABAR resulted in enhanced gabazine sensitivity in LsRDLR, the extent of this enhancement was less than that observed in ρ1 GABAR, and the enhancement was speculated to be due to the conformational changes caused by the substitutions in the orthosteric site. Docking simulations revealed that both the iminodihydropyridazine and phenyl groups of gabazine were well-accommodated in the region surrounded by several aromatic amino acid residues, such as F65, Y157, and Y205 (the so-called "aromatic box"),[11,33] in the orthosteric site of $\alpha1\beta2\gamma2$ GABAR, but not in the orthosteric site of LsRDLR. To develop highly effective competitive antagonists against insect RDLRs, it may be necessary to design compounds that utilize the aromatic pocket for stable binding. Because the orthosteric site of LsRDLR resembles, but is not the same as, that of ρ1 GABAR, structure-based design using our findings may provide a unique opportunity to develop novel, selective competitive antagonist insecticides.

Acknowledgements

We thank Dr. M. M. Rahman (Jagannath University, Bangladesh) for his previous contribution to our gabazine work. This work was supported by the National Natural Science Foundation of China (22177090).

Electronic supplementary materials

The online version of this article contains supplementary materials (Supplemental Fig. S1, S2 and Supplemental Table S1), which are available at https://www.jstage.jst.go.jp/browse/jpestics/.

References

1) N. G. Bowery and T. G. Smart: GABA and glycine as neurotransmitters: A brief history. *Br. J. Pharmacol.* **147**(Suppl 1), S109–S119 (2006).
2) M. Watanabe, K. Maemura, K. Kanbara, T. Tamayama and H. Hayasaki: GABA and GABA receptors in the central nervous system and other organs. *Int. Rev. Cytol.* **213**, 1–47 (2002).
3) M. Farrant and Z. Nusser: Variations on an inhibitory theme: Phasic and tonic activation of $GABA_A$ receptors. *Nat. Rev. Neurosci.* **6**, 215–229 (2005).
4) P. S. Miller and T. G. Smart: Binding, activation and modulation of Cys-loop receptors. *Trends Pharmacol. Sci.* **31**, 161–174 (2010).
5) J. Simon, H. Wakimoto, N. Fujita, M. Lalande and E. A. Barnard: Analysis of the set of $GABA_A$ receptor genes in the human genome. *J. Biol. Chem.* **279**, 41422–41435 (2004).
6) S. D. Buckingham, P. C. Biggin, B. M. Sattelle, L. A. Brown and D.

B. Sattelle: Insect GABA receptors: Splicing, editing, and targeting by antiparasitics and insecticides. *Mol. Pharmacol.* **68**, 942–951 (2005).
7) D. Lee, H. Su and D. K. O'Dowd: GABA receptors containing Rdl subunits mediate fast inhibitory synaptic transmission in *Drosophila* neurons. *J. Neurosci.* **23**, 4625–4634 (2003).
8) Y. Ozoe: γ-Aminobutyrate- and glutamate-gated chloride channels as targets of insecticides. *Adv. Insect Physiol.* **44**, 211–286 (2013).
9) T. Nakao, S. Banba, M. Nomura and K. Hirase: Meta-diamide insecticides acting on distinct sites of RDL GABA receptor from those for conventional noncompetitive antagonists. *Insect Biochem. Mol. Biol.* **43**, 366–375 (2013).
10) M. Asahi, M. Kobayashi, T. Kagami, K. Nakahira, Y. Furukawa and Y. Ozoe: Fluxametamide: a novel isoxazoline insecticide that acts *via* distinctive antagonism of insect ligand-gated chloride channels. *Pestic. Biochem. Physiol.* **151**, 67–72 (2018).
11) S. Masiulis, R. Desai, T. Uchański, I. Serna Martin, D. Laverty, D. Karia, T. Malinauskas, J. Zivanov, E. Pardon, A. Kotecha, J. Steyaert, K. W. Miller and A. R. Aricescu: $GABA_A$ receptor signalling mechanisms revealed by structural pharmacology. *Nature* **565**, 454–459 (2019).
12) K. Narusuye, T. Nakao, R. Abe, Y. Nagatomi, K. Hirase and Y. Ozoe: Molecular cloning of a GABA receptor subunit from *Laodelphax striatella* (Fallén) and patch clamp analysis of the homo-oligomeric receptors expressed in a *Drosophila* cell line. *Insect Mol. Biol.* **16**, 723–733 (2007).
13) G. Liu, Y. Wu, Y. Gao, X. Ju and Y. Ozoe: Potential of competitive antagonists of insect ionotropic γ-aminobutyric acid receptors as insecticides. *J. Agric. Food Chem.* **68**, 4760–4768 (2020).
14) A. N. Jain: Surflex: fully automatic flexible molecular docking using a molecular similarity-based search engine. *J. Med. Chem.* **46**, 499–511 (2003).
15) A. N. Jain: Scoring noncovalent protein–ligand interactions: A continuous differentiable function tuned to compute binding affinities. *J. Comput. Aided Mol. Des.* **10**, 427–440 (1996).
16) T. A. Pham and A. N. Jain: Parameter estimation for scoring protein–ligand interactions using negative training data. *J. Med. Chem.* **49**, 5856–5868 (2006).
17) J. J. Kim, A. Gharpure, J. Teng, Y. Zhuang, R. J. Howard, S. Zhu, C. M. Noviello, R. M. Walsh Jr., E. Lindahl and R. E. Hibbs: Shared structural mechanisms of general anaesthetics and benzodiazepines. *Nature* **585**, 303–308 (2020).
18) T. Sander, B. Frølund, A. T. Bruun, I. Ivanov, J. A. McCammon and T. Balle: New insights into the $GABA_A$ receptor structure and orthosteric ligand binding: Receptor modeling guided by experimental data. *Proteins* **79**, 1458–1477 (2011).
19) E. Sigel, R. Baur, S. Kellenberger and P. Malherbe: Point mutations affecting antagonist affinity and agonist dependent gating of $GABA_A$ receptor channels. *EMBO J.* **11**, 2017–2023 (1992).
20) S. Zhu, C. M. Noviello, J. Teng, R. M. Walsh Jr., J. J. Kim and R. E. Hibbs: Structure of a human synaptic $GABA_A$ receptor. *Nature* **559**, 67–72 (2018).
21) M. P. Goldschen-Ohm, D. A. Wagner and M. V. Jones: Three arginines in the $GABA_A$ receptor binding pocket have distinct roles in the formation and stability of agonist- *versus* antagonist-bound complexes. *Mol. Pharmacol.* **80**, 647–656 (2011).
22) J. H. Holden and C. Czajkowski: Different residues in the $GABA_A$ receptor α_1T60-α_1K70 region mediate GABA and SR-95531 actions. *J. Biol. Chem.* **277**, 18785–18792 (2002).
23) A. J. Boileau, J. G. Newell and C. Czajkowski: $GABA_A$ receptor β2 Tyr^{97} and Leu^{99} line the GABA-binding site. Insights into mechanisms of agonist and antagonist actions. *J. Biol. Chem.* **277**, 2931–2937 (2002).
24) J. H. Kloda and C. Czajkowski: Agonist-, antagonist-, and benzodiazepine-induced structural changes in the α_1Met^{113}–Leu^{132} region of the $GABA_A$ receptor. *Mol. Pharmacol.* **71**, 483–493 (2007).
25) J. G. Newell and C. Czajkowski: The $GABA_A$ receptor α_1 subunit Pro^{174}–Asp^{191} segment is involved in GABA binding and channel gating. *J. Biol. Chem.* **278**, 13166–13172 (2003).
26) D. A. Wagner and C. Czajkowski: Structure and dynamics of the GABA binding pocket: a narrowing cleft that constricts during activation. *J. Neurosci.* **21**, 67–74 (2001).
27) A. M. Hosie and D. B. Sattelle: Agonist pharmacology of two *Drosophila* GABA receptor splice variants. *Br. J. Pharmacol.* **119**, 1577–1585 (1996).
28) M. M. Naffaa, S. Hung, M. Chebib, G. A. R. Johnston and J. R. Hanrahan: GABA-ρ receptors: Distinctive functions and molecular pharmacology. *Br. J. Pharmacol.* **174**, 1881–1894 (2017).
29) R. H. ffrench-Constant, T. A. Rocheleau, J. C. Steichen and A. E. Chalmers: A point mutation in a *Drosophila* GABA receptor confers insecticide resistance. *Nature* **363**, 449–451 (1993).
30) S. D. Buckingham, B. Hue and D. B. Sattelle: Actions of bicuculline on cell body and neuropilar membranes of identified insect neurons. *J. Exp. Biol.* **186**, 235–244 (1994).
31) J. Zhang, F. Xue and Y. Chang: Structural determinants for antagonist pharmacology that distinguish the ρ1 $GABA_C$ receptor from $GABA_A$ receptors. *Mol. Pharmacol.* **74**, 941–951 (2008).
32) J. A. Ashby, I. V. McGonigle, K. L. Price, N. Cohen, F. Comitani, D. A. Dougherty, C. Molteni and S. C. R. Lummis: GABA binding to an insect GABA receptor: A molecular dynamics and mutagenesis study. *Biophys. J.* **103**, 2071–2081 (2012).
33) J. J. Kim and R. E. Hibbs: Direct structural insights into $GABA_A$ receptor pharmacology. *Trends Biochem. Sci.* **46**, 502–517 (2021).